

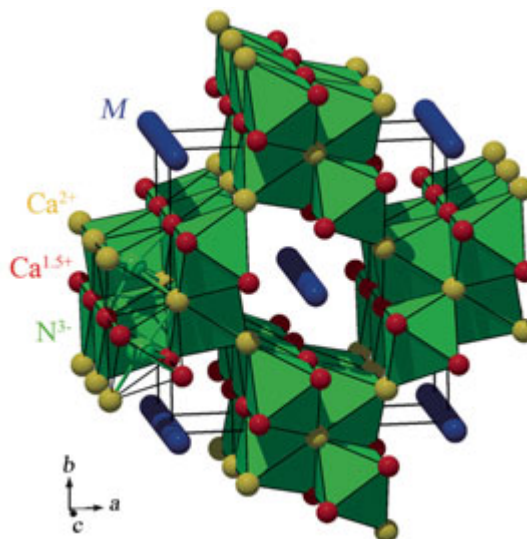
$(\text{Ca}_7\text{N}_4)[\text{M}_x]$ ($M = \text{Ag, Ga, In, Tl}$) — $\frac{1}{\infty}$ Metal Chains in Subnitrides

Peter Höhn, Reiner Ramlau, Helge Rosner, Walter Schnelle, and Rüdiger Kniep

A large number of ternary nitrides of the alkaline-earth metals (*EA*) with main group or transition elements contains “isolated” nitride ions which are exclusively octahedrally coordinated by alkaline-earth metals. Condensation of these coordination polyhedra (NE_6)⁹⁺ via common corners and edges leads to zero-, one-, two-, or three-dimensional units forming structural cavities which contain the main group and transition metal species [1] in various homo- or heteronuclear interconnections.

Ternary nitrides with composition $(\text{Ca}_7\text{N}_4)[\text{M}_x]$ ($M = \text{Ag, Ga, In, Tl}$; Fig. 1) have first been investigated in the late 1990s [2,3]. Recent re-examinations [4] led to the interpretation of the Ca/N partial structure as a subnitride $(\text{Ca}_3^{2+}\text{Ca}_4^{1.5+}\text{N}_4^{3-})^0$ (Fig. 2). Compact 2×2 chains of edge and corner sharing octahedra are connected via common apices to a three dimensional neutral framework that contains large channels of rhombic cross section (Fig. 3). X-ray diffraction investigations in combination with chemical analyses give no evidence of homogeneity ranges regardless of the system. The shape and cross section of the channels depends on the metal species incorporated, i.e. they are of more rectangular shape with increasing metal size (Fig. 3), whereas the Ca/N building blocks remain unchanged. The assignment of atomic charges in the subnitride partial structure was implemented in analogy to the procedure in subnitrides and diazenides of strontium [5] and results in a zero total charge of the subnitride partial structure. Therefore, the chains of the metal atoms within the channels have to be uncharged as well.

Compared to other calcium-nitrogen compounds with group 11 or 13 elements [6,7] there is one important difference concerning compositions and accuracy of the crystal structure determinations: for $(\text{Ca}_7\text{N}_4)[\text{M}_x]$ compounds precise determination of positional parameters for the *M* atoms is difficult as it is virtually impossible to refine preferred positions from diffraction data. Judging from electron density calculations, the stoichiometric index *x* of the in-channel positions depends on the size of the *M* atoms and decreases with increasing metal size



	Ag	Ga	In	Tl
Color	gold	bronze	bronze	gold
<i>x</i>	1.35	1.34	1.04	0.88
<i>a</i> (pm)	1143 – 1168			
<i>b</i> (pm)	1199 – 1213			
<i>c</i> (pm)	365	364	364	363
<i>d</i> (<i>M</i> - <i>M</i> , pm)	271	271	350	412

Fig. 1: Crystal structure of $(\text{Ca}_7\text{N}_4)[\text{M}_x]$. Ca^{2+} and $\text{Ca}^{1.5+}$ species and their positions are emphasized. The charge assignment is based on comparison with the crystal structures of Ca_3N_2 and Ca_2N , respectively.

Table: Unit cell parameters (space group *Pbam*) and stoichiometric indices *x* for $(\text{Ca}_7\text{N}_4)[\text{M}_x]$.

(Ag: $x = 1.35$, Ga: $x = 1.34$, In: $x = 1.04$, Tl: $x = 0.88$). This is attributed to the presence of infinite linear chains of equidistant metal atoms (Ga: $d = 271$ pm, Ag: $d = 271$ pm) occupying the centers of the channels. For In ($d = 350$ pm) and Tl ($d = 412$ pm), there is strong evidence that only chain fragments are present within the channels. The bond distances in the metal chains are incommensurate with the Ca/N partial structure. In addition, no structural correlation between different neighboring chains has been observed. This interpretation emerges from electron diffraction investigations, *ab-initio* electronic structure calculations, and transport properties measurements.

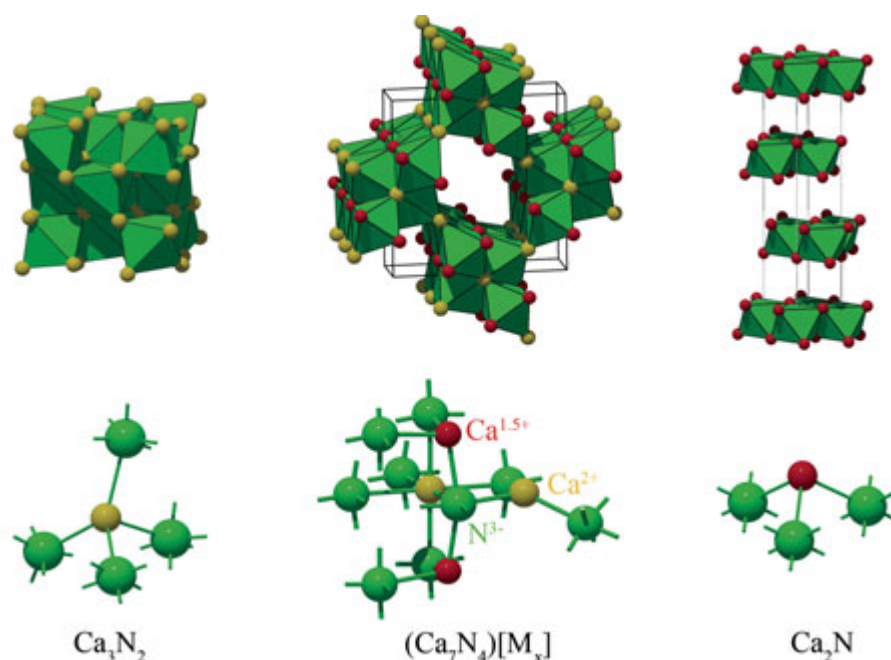
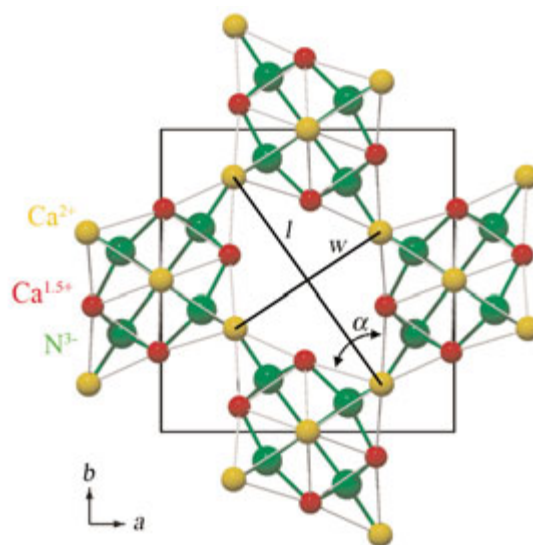


Fig. 2: Ca/N coordination in Ca_3N_2 , $(\text{Ca}_7\text{N}_4)[\text{M}_x]$, and Ca_2N , and its effect on the oxidation state of Ca.

High-resolution electron microscopy (HREM) and electron diffraction (ED) seemed to be promising tools to obtain more information about the positions of the M atoms within the channels. However, all representatives of the $(\text{Ca}_7\text{N}_4)[\text{M}_x]$ family readily hydrolyze when exposed to air and have to be prepared and transferred to the electron microscope under inert gas atmosphere. Due to the sensitivity against moisture and air, only one compound of the family, $(\text{Ca}_7\text{N}_4)[\text{Ag}_x]$, was amenable to ED experiments. High quality HREM imaging was not possible at all.

The Tecnai G² F30 electron microscope ($C_S = 1.2$ mm) with field emission gun was operated at 300 kV. Selected area electron diffraction (SAED) patterns were registered on photographic film and by means of a Gatan US-CCD camera (2048×2048 pixels). Micro-crystallites appropriate for ED were prepared in a glove box (argon atmosphere) by finely crushing the polycrystalline compound. The specimens were mounted on standard sample holders and transferred to the microscope as described elsewhere [8].

Selected-area ED patterns were registered for the [100], [110], and [010] zones (Fig. 4). In all three zones continuous diffuse lines can be discerned besides the Bragg reflections of the subnitride and of some hydrolysis product. Reconstruction in three dimensional reciprocal space results in sheets



	$\text{Ag}_{1.35}$	$\text{Ga}_{1.34}$	$\text{In}_{1.04}$	$\text{Tl}_{0.88}$
c (pm)	365	364	364	363
w (pm)	682	698	733	769
l (pm)	1005	992	969	948
α (°)	68.3	70.3	74.2	78.1

Fig. 3: Ca/N partial structure. The shape of the channel is specified by the aperture angle α and the diagonals l and w of the rhombic cross section.

Table: Values for α , c , l , and w versus the metal atom type.

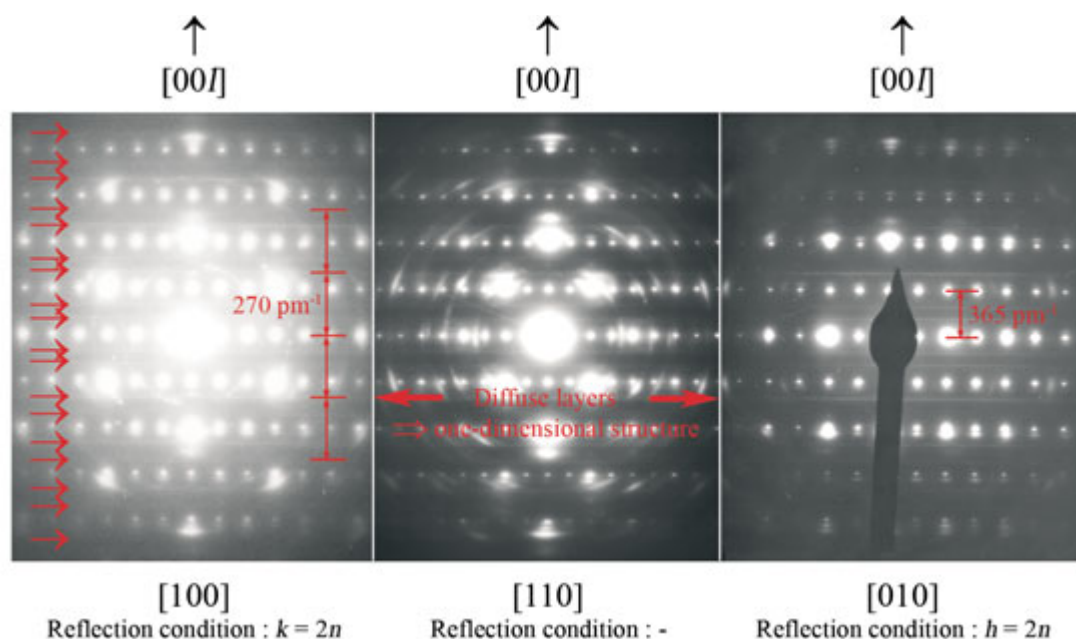


Fig. 4: SAED patterns of $(\text{Ca}_7\text{N}_4)\text{Ag}_x$ in $[100]$ (left), $[110]$ (center), and $[010]$ (right) orientation taken from different microcrystals. All three patterns show continuous diffuse lines which extend orthogonally to c^* . They appear as first-order “satellites” to the subnitride Bragg-reflections at a distance $|q| = \gamma \cdot |c^*|$ with $\gamma = 1.357 \pm 0.025$. For further details see text. The textured rings are attributed to some hydrolyzation product of the air and moisture sensitive compound. The reason for the splitting of Bragg reflections (additional satellites?) is still unknown.

of diffuse intensity $\mathbf{G} \pm \varepsilon \cdot \mathbf{a}^* \pm \eta \cdot \mathbf{b}^* \pm \gamma \mathbf{c}^*$, with ε , η being continuous and $\gamma = 1.357(25)$, which appear as first-order “satellites” to the subnitride Bragg-reflections $\mathbf{G} = [hkl]^*$. Very weak second-order satellite lines are also present. This proves that *i*) the Ag atoms form equidistant chains with $d(\text{Ag}-\text{Ag}) = 270(5)$ pm; *ii*) the chains are incommensurate to the subnitride partial structure; and *iii*) there is no correlation between the z coordinates of Ag atoms (chains) in different channels, i.e. the Ag chains are arbitrarily shifted along the channels, see e.g. [9]. It cannot be definitely concluded that the chains are infinite; they might be interrupted by vacancies. Fragmentation could lead to phase shifts between the different segments of a chain and, consequently, to a loss of correlation – even along one single channel. From the ED result for $d(\text{Ag}-\text{Ag})$, the composition of the compound is derived to be $x = 1.36$, which corresponds well to the originally weighted-in quantities, the results of chemical analysis ($x = 1.35$) and X-ray diffraction investigations, and the electronic structure calculations.

To get deeper insight in the behavior of the M guest substructure, full potential electronic structure calculations using the FPLO code [10] were carried out. The incommensurate host-guest-arrangement and the missing correlation between the M guest

chains suggest a quasi one-dimensional behavior. To check this hypothesis, we simulated the guest substructure by free, infinite one-dimensional M chains. The optimization of the in-chain bonding distance via the total energy (Fig. 5) yields 266 pm, 278 pm, 305 pm, and 317 pm for Ag, Ga, In, and Tl, respectively. For Ag and Ga, this is in very good agreement with the experimental data (271 pm for both, see Fig. 31, Table), confirming the picture of metallic, one-dimensional M guest chains in the Ca_7N_4 host lattice. For In and Tl, the calculated bonding distances are much shorter than the experimental distances under the assumption of equidistant chains (350 pm and 412 pm, respectively). This suggests a picture of M - M -chain segments in the channels with a length according to the observed stoichiometry. Such an arrangement would exhibit a small gap and, therefore, activated electronic conduction. Thus, for all M , the expected behavior is consistent with the transport properties described in the next section.

The powder samples of all four compounds show a paramagnetic susceptibility (Fig. 6). The susceptibilities are interpreted as the sums of weakly temperature-dependent paramagnetic contributions and low-temperature upturns from Curie-like impurities. Thus, the four compounds are Pauli-

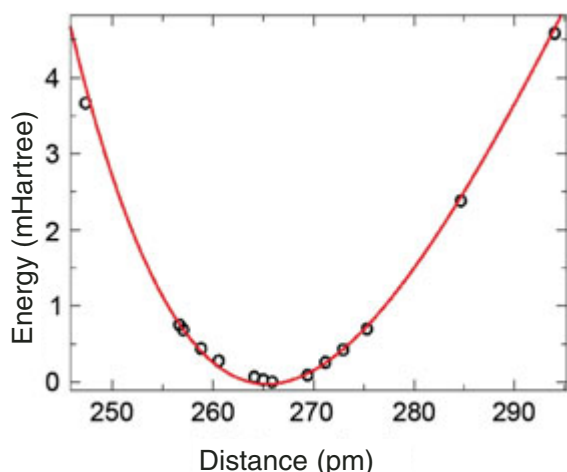


Fig. 5: Energy versus bond distance for a one-dimensional equidistant chain of Ag atoms. The red line is a fourth-order fit to the calculated data. The energy of the minimum at 266 pm is set to zero.

paramagnetic metals with occupied states at the Fermi level E_F . The weakly T -dependent Pauli-paramagnetic contribution χ_p and the diamagnetic core contributions χ_{dia} can not be separated easily, however, we estimate $\chi_p \approx 300 \times 10^{-6} \text{ emu mol}^{-1}$ for the Ag and In compounds. This corresponds to a density of states $N(E_F) = 9\text{--}10 \text{ states eV}^{-1} \text{ f.u.}^{-1}$. For the compounds with $M = \text{Ga}$, Tl about half the density of states is estimated.

The electrical resistivities $\rho(T)$ (Fig. 7) of the four compounds, however, are quite different: The Ag compound clearly displays a linear temperature dependence and a room temperature resistivity around $10^{-3} \Omega \text{ cm}$ indicating a (bad) metallic conduction. The resistivity of the Ga compound is

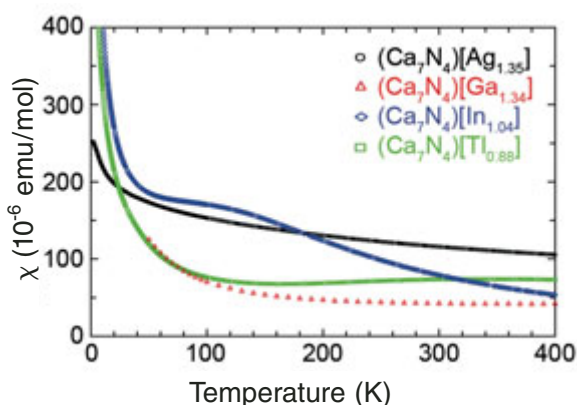


Fig. 6: High-field magnetic susceptibility $\chi = H/M$ versus temperature T . The data were measured at $\mu_0 H = 7 \text{ T}$ and were corrected for ferromagnetic impurities.

metallic (increases with temperature) above ca. 30 K but shows a weak upturn below this temperature. The compounds with In and Tl exhibit a thermally activated conduction mechanism. It has to be kept in mind that in powder samples the metallic chains of the crystallites are interrupted and separated by high-resistivity material, thus increasing the overall resistivity. Interestingly, in the In and Tl compounds the metal chains are additionally interrupted on the atomic scale. Simple statistics suggest that – with the given compositions and equilibrium distances of the M atoms – average chain lengths of 2.42 nm and 1.39 nm for $M = \text{In}$ and Tl, respectively, are achieved. A closer inspection of the temperature dependence of $1/\rho$ of these samples reveals that their conduction mechanism can be described well by three-dimensional variable range hopping with an exponent $\gamma = 1/4$, as could be expected for an ensemble of segmented conducting chains. Only the Ag compound behaves like a metal compatible with atomically uninterrupted M chains. The high value of the room temperature resistivity is then a result of bad electrical contacts between the crystallites of the sample.

In conclusion, in the ternary nitrides with composition $(\text{Ca}_7\text{N}_4)[M_x]$ uncharged metal chains ($M = \text{Ag}$, Ga) or fragments thereof ($M = \text{In}$, Tl) are located within channels of a 3D Ca/N subnitride partial structure.

Physical properties investigations and electronic properties calculations give conclusive results for the occupancy x . Whereas the compounds with $M = \text{Ag}$, Ga are metallic, thermally activated conduction behavior is found for $M = \text{In}$, Tl.

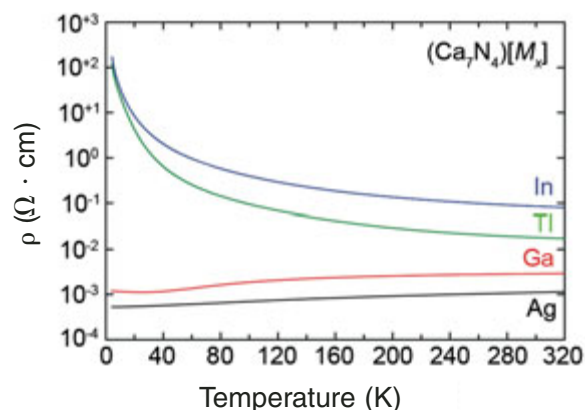


Fig. 7: Electrical resistivities ρ versus temperature T for cold-pressed powder samples of $(\text{Ca}_7\text{N}_4)[M_x]$. The measurements were performed by the van-der-Pauw method in a die cell made of pure sapphire [8].

The authors wish to thank *Gudrun Auffermann*, *Ulrike Schmidt*, and *Anja Völzke* for chemical analyses.

References

- [1] *P. Höhn and R. Kniep*, *Z. Anorg. Allg. Chem.* **628** (2002) 2174.
- [2] *M. Ludwig*, Dissertation, TU Darmstadt 1998.
- [3] *J. Jäger*, Dissertation, TU Darmstadt, 1995.
- [4] *P. Höhn, R. Ramlau, H. Rosner, W. Schnelle, and R. Kniep*, *Z. Anorg. Allg. Chem.* **630** (2004) 1704.
- [5] *Y. Prots, G. Auffermann, M. Tovar, and R. Kniep*, *Angew. Chem. Int. Ed. Engl.* **41** (2002) 2288.
- [6] *M. Kirchner, W. Schnelle, F. R. Wagner, R. Kniep, and R. Niewa*, *Z. Anorg. Allg. Chem.* **631** (2005) 1477.
- [7] *O. Reckeweg, T. P. Braun, F. J. DiSalvo, and H. J. Meyer*, *Z. Anorg. Allg. Chem.* **626** (2000) 62.
- [8] *W. Schnelle, U. Burkhardt, R. Ramlau, R. Niewa, and G. Sparn*, Scientific Report 2001/2002, MPI-CPfS, Dresden 2003, p. 38.
- [9] *F. Frey*, *Acta Crystallogr.* **B51** (1995) 592.
- [10] *K. Koepernik and H. Eschrig*, *Phys. Rev. B* **59** (1999) 1743.